

12
AD-A278 440



**Plasma Physics Applications to Intense Radiation Sources,
Pulsed Power and Space Physics
Short Pulse Ultra Intense Laser-Plasma Interaction Experiment**

Final Technical Report on NRL Grant # N00014-90-J-2002

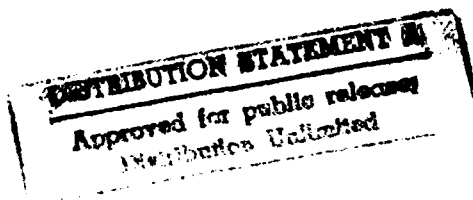
Period: January 1, 1990 - May 31, 1993

Technical Monitor:

Dr. Sidney Ossakow

Principal Investigator:

Prof. R.N. Sudan



94-11974



DTIC QUALITY INSPECTED 3

94 4 20 005

This report covers the activities engaged by members of the Laboratory of Plasma Studies, Cornell University under NRL Grant # N00014-90-J-2002 for the period January 1, 1990 to May 31, 1993.

Personnel

The personnel supported in part by this Grant are listed below:

Principal Investigator

Professor R.N. Sudan

Co-Principal Investigator

Professor D.A. Hammer

Postdoctoral/Research Associates

J.B. Greenly, Sr. Research Associate

N. Qi

K.C. Mittal

G. Rondeau

Graduate Research Assistants

D. Kalantar

D. Longcope

L. Adler

M. Rilee

Accession For	
NTIS GRA&I	<input checked="" type="checkbox"/>
DTIC TAB	<input type="checkbox"/>
Unannounced	<input type="checkbox"/>
Justification	
By <i>per letter</i>	
Distribution/	
Availability Codes	
Dist	Avail and/or Special
<i>A-1</i>	

Technical Progress Accomplished (1/1/90 - 5/31/93)

The work accomplished is divided into four parts. The abstracts of the papers published in the topics covered by radiation physics, ultra-intense lasers and the ultra-intense laser laboratory are given below. The fourth part is the report on work accomplished under

the sub-project on "Magnetically Enhanced Gas Switch Experiments". The abstracts of conference papers are appended.

I. Radiation Physics

1. "Characterization of X-Ray Emission from Aluminum X-Pinch Plasmas Driven by the 0.5 TW Lion Accelerator", N. Qi, D.A. Hammer, D.H. Kalantar and G.D. Rondeau, *J. Quant. Spectrosc. Radiat. Transfer* Vol. 44, No. 5/6, pp. 519-527, 1990.

Abstract

Intense bright x-ray sources from dense z-pinch and x-pinch plasmas are being investigated for photo-pumping x-ray laser media. Crossed Al wire X-pinchs with mass line density up to hundreds of micrograms per centimeter have been imploded by up to 600 kA current for 40 ns using a 0.5 TW pulsed power generator. High density bright spots are observed. Soft x-ray spectroscopy was used to infer plasma density of up to $\sim 10^{20} \text{ cm}^{-3}$, and temperature of 100 -300 eV. The optimum mass loading for different ionization stages of Al ions was examined. Parallel wire z-pinchs yielded both lower density up to $\sim 10^{19} \text{ cm}^{-3}$, and lower temperatures (70 - 200 eV), than the X-pinch plasmas.

2. "Neutron Production in Dense X-Pinch Plasmas Produced from Deuterated Polyethylene Fibers", K.C. Mittal, D.H. Kalantar, N. Qi, D.A. Hammer, K.A. Gerber and J.D. Sethian, *J. Appl. Phys.* 70 (11), 1 December 1991.

Abstract

A novel intense source of 2.45 MeV neutrons is described. Exploratory experiments with deuterated polyethylene fibers in an x-pinch configuration have been performed using 370-kA, 80-ns current pulses. Up to 4.5×10^8 neutrons per pulse have been produced. Compared to a z pinch, an x pinch produced about the same number of neutrons for the same current, but the x-pinch neutron source may be 1 mm or less



LABORATORY OF PLASMA STUDIES

Cornell University

369 UPSON HALL
ITHACA, NY 14853-7501

(607) 255-4127
(607) 255-3004 (Fax)

March 22, 1994

Dr. Sidney Ossakow, Technical Monitor
Naval Research Laboratory
Plasma Physics Division, 6700
4555 Overlook Ave., SW
Washington, DC 20375-5000

Dear Dr. Ossakow:

Please find enclosed 2 copies of the Final Technical Report on the research work performed by scientists of the Laboratory of Plasma Studies, Cornell University under NRL Grant # N00014-90-J-2002. Please feel free to contact me if you have any comments.

Sincerely,

R.N. Sudan
Principal Investigator

Enclosures

cc: Admin. Contracting Officer, NRL
Director, NRL
✓ Defense Technical Information Center

RNS/scj

in diameter.

3. "Fluorescence in Mg IX Emission at 48.340 Å from Mg Pinch Plasmas Photopumped by Al XI Line Radiation at 48.338 Å" N. Qi, D.A. Hammer, D.H. Kalantar and K.C. Mittal, *Phys. Rev. A* Vol. 47, No. 3, March 1993.

Abstract

Resonant photopumping of Be-like Mg IX ions by Li-like Al XI line radiation has been studied in pulsed-power-driven plasmas as a possible approach to achieve laser action in the extreme-ultraviolet wavelength region. An Al x-pinch or z-pinch plasma imploded by a 0.5-TW pulsed power generator produced intense line radiation at 48.338 Å. A separate Mg z-pinch plasma, driven by the same pulsed power generator, was created in parallel with 1 cm separating the two plasmas. Evidence for fluorescence (resonant scattering) was the appearance of 48.340-Å resonance line emission from the 4p level of Mg IX ions due to photopumping by the Al XI line radiation at 48.338 Å. Fluorescence may also have been observed on the Mg VIII line at 52.395 Å, photopumped by Al XI line radiation at 52.446 Å. Both Al and Mg plasmas were characterized in the experiments. Improvements to the pump geometry required to achieve gain on the Mg IX line at 228 Å are also discussed.

The work under 2 and 3 was jointly supported by NRL and Sandia National Laboratories, Albuquerque, NM.

II. Ultra Short Ultra Intense Laser Plasma Interaction

1. "Two-Dimensional Self-Focusing of Short Intense Laser Pulse in Underdense Plasma", X.L. Chen and R.N. Sudan, *Phys. Fluids B* 5 (4), April 1993.

Abstract

A simplified set of three-dimensional equations are derived for the propagation of an intense laser pulse of arbitrary strength $a = eA/mc^2$

(where \mathbf{A} is the magnetic vector potential of the laser pulse) in cold underdense plasma. In different limits, the equations can be easily reduced to those of previous one-dimensional models [Phys. Fluids **30**, 526 (1987); Phys. Rev. A **40**, 3230 (1989); **41**, 4463 (1990)]. For $|a| < 1$, an approximate set of equations from the averaged Lagrangian is obtained. The present study differs from previous work in that wave dispersion is also important for short laser pulse, and is included in the model equations. The axisymmetric two-dimensional model equations are solved numerically to show the effect of dispersion in the self-focusing process.

2. "Necessary and Sufficient Conditions for Self-Focusing of Short Ultraintense Laser Pulse in Underdense Plasma", X.L. Chen and R.N. Sudan, *Phys. Rev. Lett.* Vol. 70, No. 14, April 1993.

Abstract

We analyze the propagation of a short intense laser pulse in underdense cold plasma. When no electron cavitation is present, a global invariant H is obtained, and its relation with self-focusing is studied. For relativistic self-focusing $H < 0$ is a sufficient and necessary condition. For relativistic and ponderomotive self-focusing, $H < 0$ is sufficient but not necessary. Numerical simulations are performed to confirm the above points.

3. "Mechanism for the Generation of 10^9 G Magnetic Fields in the Interaction of Ultraintense Short Laser Pulse with an Overdense Plasma Target", R.N. Sudan, *Phys. Rev. Lett.* Vol. 70, No. 20, May 1993.

Abstract

The physical mechanism for the generation of very high "dc" magnetic fields in the interaction of ultraintense short laser pulse with an overdense plasma target originates in the spatial gradients and nonsta-

tionary character of the ponderomotive force. A set of model equations to determine the evolution of the "dc" fields is derived and it is shown that the "dc" magnetic field is of the same order of magnitude as the high frequency laser magnetic field.

The work under 1, 2 and 3 was jointly supported by NRL and ONR.

III. Ultra Short Ultra Intense Laser Laboratory

This new laboratory in support of the NRL program under Dr. P. Sprangle on the same topic was initiated in early 1993 in the Laboratory of Plasma Studies.

The capital equipment funds this year were used to purchase the first of three stages of an ultra high intensity, short pulse laser system. The three stages include a mode locked oscillator, a regenerative amplifier and a high power amplifier. With this years funds we have obtained several major items including a mode locked Ti:sapphire oscillator, an ion argon pump laser, the optics for the mode locking cavity and a CCD camera. These funds were also used to acquire some smaller items which include an infrared viewer, sampling scope plug-ins, a closed cooling system for the Ti:sapphire rod, a Gateway 486 PC for controlling the CCD camera and the parts for an autocorrelator.

IV. Magnetically Enhanced Gas Switch Experiments

A. Introduction

Switches are key components of high peak power pulsed systems. A new switch concept, the "Magnetically Enhanced Gas" (MEG) switch described in Section II of this report, combines two types of switches, gas insulated spark gaps and magnetic switches (saturable core inductors), to produce a switch with attributes of both but without some of their limitations for high power short pulsewidth applications. This switch is potentially of great importance in many pulsed power applications.

As a result of potentially severe erosion problems on the main output switches of the NIKE laser at the Naval Research Laboratory (NRL), NRL has funded the MEG switch experiments described in Section III. These experiments, conducted at $\leq 70\text{kV}$, $\leq 110\text{kA}$ and 600ns pulsewidth using a trigatron switch, have shown that the MEG switch decreases the peak power and energy dissipated in the switch compared to the same switch without a series magnetic switch. We discuss the results and conclusions in Section IV.

B. The MEG Switch Concept

There are a variety of switch types available for pulsed power applications, including gas insulated spark gaps, thyratrons, saturable magnetic inductors, surface flashover switches, etc. Each has different capabilities and limitations. In particular, these limitations have increased the operating cost and down time of high peak power systems and impeded the development of high peak power repetitive rate pulse systems. These limitations have also slowed the development of pulsed power systems for industrial and commercial applications.

In this section, we will first briefly discuss spark gaps and magnetic switches and then explain the thesis behind the operation of the MEG switch. Advantages of this switch and examples of potential applications will be presented. Specifically, partial alleviation of at least one limitation of the ordinary spark gap switch will be demonstrated.

Gas insulated spark gaps¹ have been the mainstay of pulsed power technology. They are mechanically simple devices, relatively

small, lightweight and inexpensive, and can be designed to operate at very high voltages, currents and peak powers. However they have several limitations. Switch life (number of pulses) at high operating levels is limited by erosion of the electrodes and damage to insulators as a result of the energy dissipated in the switch. Repetition rate is limited both by gas recovery time (~ 10 ms) and the limited electrode lifetime. Switches have been developed to operate at high repetition rates at the expense of added complexity and external systems required to cool the switch and renew the insulating gas. The problem of limited shot life remains.

Magnetic switching (solid state switches using saturable core inductors) proposed by Melville² and pioneered by Dan Birx and others at LLNL³ have demonstrated reliable, reproducible long lifetime operation at very high repetition rates ($>100,000$ pps in bursts). These switches are particularly attractive for use in high repetition rate, high average, but moderate peak power applications. In principle, magnetic switches can be designed to operate at any level. However, the size (volume and weight) and cost of these switches is proportional to the energy switched and switch gain squared. (Switch gain can be defined as the input pulsewidth divided by the output pulsewidth for a constant peak pulse voltage.) Switch volume can be minimized by using multiple stages of compression at the expense of having to store the full pulse energy at each stage and by making the triggered stage (prior to the magnetic switches) output pulse as narrow as possible to minimize gain requirements. Even so, for moderate energy per pulse, high peak power (which implies high switch gain requirements) systems the size and cost of the magnetic switches (and additional capacitors) dwarf that of gas insulated spark gap switches.

We believe that by combining a small magnetic switch in series with a gas switch we can dramatically extend the lifetime, current capability, and repetition rate capability for switches operating in short pulse ($< \text{few } \mu\text{s}$) high current applications. The purpose of this combination is to decrease the energy dissipated in the switch and to control the way this energy is dissipated.

The thesis behind the MEG switch concept is as follows. Losses in short ($< \text{few } \mu\text{s}$) conduction time switches occur mostly early in the pulse when the current is rapidly rising and the switch channel diameter in the gas is small, resulting in a large channel resistance and substantial voltage drop. Because the current is rapidly rising,

this can result in large peak powers dissipated in the switch. Even more important is the fact that this energy is initially confined to a small channel diameter, depositing very large power density in the switch electrodes. It is during this time that the bulk of the electrode erosion probably occurs.

The addition of a saturable inductor in series with the switch serves to delay the onset of the full switch current by some fixed time. When the switch initially closes the larger inductance limits the rate of rise of the switch current to a small value. The current channel increases in diameter with time (at a rate weakly dependent on the current), and the voltage across the switch drops. When the inductor saturates and its inductance becomes negligible, the current can rise rapidly to its full value, but the power dissipated in the switch is less and is dissipated over a larger area on the electrode than in the absence of the saturable inductor. The expectation is that this will result in substantially less electrode damage or, conversely, the ability to conduct more current through a given switch at the same damage level. This also means that less debris will be deposited on the switch housing per pulse, thereby increasing cleaning interval for the switch. Another potential benefit is more rapid recovery time, which, along with lower switching losses, permits higher repetition rate operation at lower gas flow rates. Ensuring that switches operating in parallel all conduct current is also easier with the MEG switch. This is because when the earliest switch closes, the voltage is not removed from the other switches until the first inductor saturates. Care must be taken (either by having sufficient switch circuit inductance or coupling between cores) to ensure all parallel inductors saturate.

MEG switch lifetime may be further extended by using different electrode materials. For long pulse, modest di/dt switch applications, electrodes made of a high temperature material, such as graphite, provide substantially longer lifetimes than brass electrodes. For short pulse, high di/dt switches, the converse is true. This is possibly because graphite, with a relatively low thermal conductivity, is damaged by localized thermal shock (caused by the high power density on the electrode surface), whereas brass, with a higher thermal conductivity, simply melts. The MEG switch should decrease this thermal shock (by reducing the peak power density), allowing graphite electrodes to be used in short pulse applications, further extending switch lifetime.

The MEG switch would retain the simplicity of a gas switch with only a slight increase in cost and weight due to the small saturable core. Also, existing gas switches can be retrofitted with appropriately sized cores around the switch connections. In most applications the core can be located in the circuit so that the DC or pulse charging of the stage to be switched will reset the switch core. Use of the MEG switch does not introduce new failure modes as a failure of the insulation in the saturable inductor only results in the switches reverting back to normal gas switch operation.

A technique similar to the MEG concept has been used^{5,6} with thyristors to enable them to conduct high currents for short pulses which would otherwise destroy the devices. This concept has also been used to minimize electrode damage in thyratrons operating in a short pulse high current mode⁷.

In a conventional gas switch, power dissipation, which results in electrode erosion, is related to the electric field initially in the gap, among other things. The greater this field, (i.e. the smaller the gap spacing) the shorter the resistive phase and the lower the losses. However, the smaller the gap spacings are, the more pronounced are the effects of electrode erosion. The MEG switch can operate with larger gaps to minimize erosion effects without increasing the power and energy dissipated in the switch and so without increasing the erosion rate.

A few potential applications will be described here. The longer lifetime means retrofitting existing (and equipping new) Marx generators with MEG switches will decrease maintenance cost by increasing the interval (number of pulses) between switch refurbishing. The higher current capability enables retrofitting of existing Marx generators with higher energy density capacitors without building all new switches by adding the appropriate saturable inductor around the connections to the existing switches. Parallel operation with long lifetimes could improve intermediate pulseline switch performance and perhaps replace the low inductance output liquid dielectric switches (which have a short life and produce substantial mechanical shock in the pulseline). The decrease in energy dissipated in the switch, resulting in less cooling requirements (and perhaps faster recovery times), combined with long or lifetime make the MEG switch a good candidate for high power, high repetition rate applications. The switch's modest size and weight compared to the combination of thyratron and magnetic

switches required to switch the same peak power levels could make it particularly appropriate for mobile applications.

C. Experiments

Two experiments were performed to examine the feasibility of the MEG switch concept. The goal of the first was to examine the relationship between saturable inductor size (volt-second product) and the peak power and energy dissipated in the switch during its turn on phase for different switch operating parameters. The second experiment measured the switch electrode erosion after a large number of shots in order to determine if electrode lifetime is increased using saturable inductors. This section describes the experiments and Section IV presents the results.

Test Circuit

A trigatron type gas insulated spark gap in series with ferrite (Phillips 3C81) or NiFe (50% Ni, 50% Fe, .001" thick tape-wound) toroidal cores was used as the test switch. The test circuit schematics are shown in Figures 1a and 1b. For both circuits C2, the capacitor discharged by the test switch, is pulse charged. The charging current flows through the stray circuit inductance, the saturable inductor (when installed) and the load resistors, R. When the test switch closes, C2 discharges through the load resistors and saturable cores with the direction of the current opposite from that during charging. This circuit arrangement was used for several reasons. Pulse charging C2 through the saturable inductors insures sufficient current to fully reset the cores on each shot. In additions, pulse charging allows us to use a low impedance, fast risetime resistive voltage monitor for measuring the voltage at the switch. By locating one side of the test switch at ground potential, we also simplify switch voltage measurements.

The test switch, load resistors and saturable inductor was located inside an aluminum container which mounts directly on top of C2 as is depicted in Figure 2. In different experiments, the saturable inductor was made by placing a variety of different ferrite and NiFe toroidal cores around the conducting post which connects the load resistors to one side of the switch. The other switch electrode was mounted on the end plate of the aluminum container, where the Rogowski coil current monitor was also located. The trigger pin was in the center of this electrode. The load is made up of one to three 0.2 Ω disc ceramic resistors connected in series. The container was pressurized with SF6 gas at the pressure required to

insulate the switch gap. This gas also serves to insulate the rest of the output circuit. Various feed-throughs located on the side of the container were used to make the connections to the voltage monitors and the input from the charging pulser.

The compact coaxial arrangement minimized inductance and made inductance calculations (and so inductive voltage corrections) straightforward. Gas insulation, which was adequate to >60 kV using SF₆, simplified making frequent switch or saturable inductor changes. Also the hardware could be mounted on any capacitor with the same type of header, making it possible to change C2 capacitance in order to vary switch current pulsewidths and di/dt. This mechanical layout eliminated the need for an insulating switch housing which might have been damaged by the large number of high current pulses planned for these experiments.

The test switch was triggered by a -30kV pulse supplied by an SCR/magnetically switched trigger generator (Figure 3). Because of the large number of pulses and the continuous operation anticipated for these experiments, this trigger generator, anticipated to have a very long lifetime, was used instead of more common devices, such as a PT-55, which use limited lifetime krytron switches.

The initial experiments used a pulser (Figure 1a) consisting of a 0.7 μ F capacitor (C1) in series with a midplane triggered gas switch (S1) and a 100 μ H inductor to charge C2. The 100 μ H inductor isolates C1 from C2 when the test switch is fired. S1 is triggered by a PT-55. This pulser was used because it can be operated at voltages up to 60kV. However, for the lifetime experiments the pulser in Figure 1b was used because of the long lifetime of the thyratrons. This pulser consists of a dual thyatron, 3 μ F switch chassis (originally used on ETA at LLNL) charging C2 through a 3 to 1 air core step-up transformer. The transformer consists of approximately 17 primary turns of RG-8 center conductor and insulator, sandwiched between 50 secondary turns wound on a 9" diameter PVC pipe. Operating C1 at 18kV resulted in charging C2 to 44kV.

To protect the dc power supply and insure that the switches recover after C2 is discharged, the power supply is gated off just prior to each shot. A block diagram of the control system is shown in Figure 4. The operating sequence is as follows: A 5V signal from the 1pulse/minute generator triggers the master control circuit.

This circuit, which also controls charging and dumping of C1, disengages the HV power supply for ~5 seconds and, after an initial delay of 1 second, triggers the delay generators. The delay generators independently control the timing of the triggering of S1, S2 and the data acquisition system. This system was designed to operate continuously and was operated for hours at a time during the lifetime testing.

Diagnostics

Measurement of switch loss is difficult because of the large dynamic range (~70kV to <100V) required of the voltage monitor and data acquisition system. Also the inductive voltage drop adds to the apparent switch voltage. The latter can be compensated for by subtracting an $L \, di/dt$ signal from the voltage monitor signal. However, the arc inductance is difficult to measure exactly and is constantly changing in value, resulting in small errors. This can result in large errors in the calculation of switch losses during the conduction phase when the switch voltage may be < 100 volts. We avoided these difficulties for these experiments as we were concerned only with turn-on losses. During the turn-on phase, the switch voltage is still much larger than the errors introduced by the limited resolution of the voltage measurements (8 bit resolution A/D conversion) and inexact inductive voltage correction. In this case, the voltage measurement system must have a fast response time (<5ns), but does not need a large dynamic range. The value for L was determined by shorting out the switch electrodes with a 1 mm rod and pulsing a current through the switch while observing the voltage monitor output.

Resistive voltage monitors are used to measure the voltage on C2, the voltage across the switch and the voltage across the saturable inductor and switch combined. The monitors were calibrated, and a <5ns response time verified, by comparing their outputs with that of a Tektronix 40kV oscilloscope probe. A Rogowski coil was used to measure switch current.

Two optical diagnostics were used to obtain qualitative information on the power dissipated in the switch. An HP 5082-4200 PIN photodiode was used to measure the visible light intensity from the switch gap. The second detector consisted of a photomultiplier tube (PMT) with a few nanosecond response time and a Schott Glass ultraviolet filter (UG-11) to measure the risetime

and relative intensity of the UV light emitted by the spark channel. The peak sensitivity of the PMT with the filter was at a wavelength of approximately 350nm, and the 20db attenuation points were at 290nm and 400nm. Time constraints and the unavailability of a streak camera while this experiment was in progress prevented our carrying out time resolved measurements of the diameter of the spark channel, as originally planned.

The change in the mass of each electrode was measured for the electrode erosion experiments. However these results can underestimate electrode erosion rates, as material eroded from the tips of the electrodes may condense elsewhere on the electrode. The profile of each electrode magnified 10 times by a standard optical inspection comparitor was photographed from two angles before and after the electrode erosion experiments to record surface geometry changes.

The large amount of data produced by these experiments (~100 megabytes) made it essential to automate the acquisition and analysis process. The data acquisition system consisted of several channels of LeCroy 200MS/s, 8 bit digitizers controlled by National Instruments Labview II software installed in a Macintosh II computer. A Virtual Instrument (VI) was developed which transfers the data from the digitizers to the Macintosh hard drive, uses the fiducial signals to synchronize the timing, corrects for any dc offset in the digitizer used to acquire the di/dt signal, performs inductive corrections to the voltage measurements, integrates di/dt and calculates instantaneous switch power and energy dissipated in the switch. This VI also stores the raw data and displays I_{sw} , V_{sw} , P_{sw} , E_{sw} , V_{ind} and V_{PMT} (where the quantities are switch current, voltage, power, energy dissipated, saturable inductor voltage and the photomultiplier voltage, respectively) after each shot. The diagram of the VI is shown in Figure 5. Initial results presented at the 1991 Conference on Plasma Science⁸, Williamsburg, Va, and the 8th IEEE Pulsed Power Conference⁹ in San Diego, CA were based on the results generated by this VI. However, the VI shown in Figure 6 was used to analyze the data after all experiments were completed. Its input is the raw data stored by the previous VI. The analysis VI uses Labview sub-VIs to automatically correct the relative timing of the di/dt and V_{sw} signals and to determine the peak power dissipation and the energy dissipated in the switch up to the time the switch reaches peak current. Using the same analysis VI with essentially no operator adjustments for all experiments insures that the

analysis is done consistently and excludes any unintentional bias introduced by the experimentalist. The results from using this VI are presented next.

D. Results

Table 1 summarizes the results of the first set of experiments. The table was developed using the results of the analysis VI in the following manner: Results from multiple shots having the same switch circuit (capacitance, load resistance and saturable inductor) values, and with C1 charged to the same voltage were averaged. In order to compare the effects of different saturable inductors, the averaged values for a particular set of C1 charging voltage, C2 value and load resistance were then adjusted by multiplying the results by the peak switch current with no saturable inductor divided by the peak switch current with the given saturable inductor. This ratio ranged from 0.98 to 1.05. Figure 7 shows typical (voltage and current) signal waveforms for the switch both with and without a saturable inductor. In the next few paragraphs, these results are discussed.

Figure 8 shows a plot of peak switch power as a function of the peak switch current. It can be seen that in every case there is at least one size of saturable inductor which results in lower peak power dissipation in the switch. It also is apparent that the decrease is only weakly dependent on the size of the saturable inductor volt-second product, and that too large of an inductor may result in little or no improvement. For example, at 94kA doubling the size of the inductor, which increased the turn-on delay to 65ns (from 32ns), caused a further decrease in peak power dissipation by only 16% and resulted in slightly higher switch losses than with the smaller inductor. The relatively small size of these inductors used here (1kg of 50% Ni 50% Fe material) implies that the inductors required for higher current and voltage applications will not be impractically large or add substantially to the switch inductance when in the saturated state. Further testing at higher currents is necessary to confirm this.

Figure 9 shows a plot of energy dissipated in the switch up to the time the current reaches its peak value, as a function of peak switch current. Figure 10 is similar, except the energy dissipated in the switch is expressed as a percentage of the energy in C2. Lines are drawn connecting data points having similar switch voltages.

Two observations can be made for the case of no saturable inductor. First, at the same switch voltage, and thus same electric field in the gap, the losses increase as the current increases. However, as the electric field in the gap is increased, the percentage of loss in the switch decreases. This is expected as the duration of the resistive phase, t_r , for short pulse gas switches is¹⁰:

$$t_r = (p/p_o)^{1/2} \times 88 / (Z^{1/3} \times E^{4/3}) \text{ ns}$$

where p/p_o is the switch gas density relative to the density of air at one atmosphere, Z is the source impedance and E is the electric field in MV/m. Increasing the electric field decreases the duration of the resistive phase and thus decreases switch losses. The fact that our results show this behavior increases our confidence in the validity of our diagnostic/data analysis technique. When saturable inductors are used, the energy loss in percent is relatively constant as the current increases and there is no clear relationship between losses and electric field in the gap. The latter result indicates that a substantial amount of the turn-on process occurs prior to inductor saturation, while the switch gap voltage is small and the same regardless of the initial switch voltage. (Most of the voltage drop is across the saturable inductor at this time.) The UV PMT signals (Figure 11) show the differences in the turn-on process qualitatively, a few nanosecond risetime light signal for no inductor versus a ~ 100 ns risetime with a saturable inductor. We have neglected losses in the saturable inductors as this will be less than 1 joule /pulse at the highest current levels.

Lifetime Experiments

The lifetime experiments were conducted at 45kV and 46kA, which was the maximum reliably attainable using the thyatron switch chassis. At the time the lifetime experiments were undertaken, the initial data from earlier experiments indicated a substantial decrease in peak power and energy dissipation using saturable inductors at this current level. However the results obtained by analyzing the data with the analysis VI shows a much smaller difference (see Figures 8 & 9) and indicate that a smaller size saturable inductor may have been more effective. Because of this, many more shots than the $\sim 2,000$ /switch from the lifetime experiments are needed to produce conclusive results. However we will summarize our results here. The average change in mass for the trigger side electrode was 127 μ g/ pulse with no saturable inductor

and $94\mu\text{g/pulse}$ with a 2.9×10^{-3} volt-second inductor. The values for the opposite electrode were $43\mu\text{g}$ without and $41\mu\text{g}$ with the inductor.

Before and after photographs showing the contour of the trigger side electrode from the switch which used a 2.9×10^{-3} volt-second inductor, magnified 10 times, are presented in Figure 12. The height of the largest features is $\sim 100\mu\text{m}$. The switch electrodes from testing without the saturable inductor show similar results.

E. Summary

In summary, the following conclusions can be made:

1) Using a saturable inductor in series with a spark gap decreases the peak power dissipation and the switch energy loss during the turn-on phase.

2) For the same electric field in the switch gap, the effectiveness of this combination improves as the switch current and di/dt rate increased.

3) Decreases in the energy dissipated in the switch can be obtained by operating with higher electric fields in the switch gap, without using a saturable inductor. Thus, by operating with smaller gap spacings, losses in a standard switch can be decreased to the level of the MEG switch. However, the smaller gap spacing means that detrimental effects of electrode erosion on switch operation will occur much sooner. Thus increasing the electric field in the gap may result in no improvement in switch lifetime for a standard switch.

4) Increasing the electric field in the switch gap has no clear effect on the MEG switch losses. The apparent lack of a relationship between the initial switch voltage and the relative switch loss for the MEG switch indicates that a substantial fraction of the resistive phase of switch turn-on occurs before the inductor saturates.

5) Slightly lower electrode erosion was observed using the MEG switch during the lifetime experiments. However, many more

shots or testing at higher currents is needed to determine if the MEG switch combination will substantially increase switch lifetimes.

6) The inductors required for higher current and voltage applications will not be impractically large or add substantially to the switch inductance when in the saturated state.

7) The lower peak powers dissipated in the MEG switch may permit materials such as graphite, which can be damaged by thermal shock, to be used in short pulse applications.

Further experiments using the appropriate switches operating at higher currents and voltages are needed to determine if the MEG switch concept will be useful for the applications described at the end of Section II. Based on the results presented here, we believe these experiments are worth pursuing.

Abstract Submitted for the Thirty-second Annual Meeting
(Division of Plasma Physics)
November 12-16, 1990

Category Number and Subject 5.10

 Theory X Experiment

"Flashboard Plasma Characterization by Framing Photography and Emission Spectroscopy," A. BEN-AMAR BARANGA, D.A. HAMMER, J.B. GREENLY, L.K. ADLER and N. QI, Cornell University,* - The plasma produced by an NRL 6cm \times 10cm flashboard plasma gun has been investigated by framing photography and emission spectroscopy. The flashboard has been tested with the 6 chains connected to ground through separate 100nh inductors. A uniform, directed flow of plasma perpendicular to the flashboard with speed 10cm/ μ sec was observed. Doppler broadening of emission lines implied 1.5cm/ μ sec transverse velocity. The plasma ion density was $1-2 \times 10^{13}/\text{cm}^2$. It is mostly C^+ and C^{++} and its temperature is 3-4eV. In a second configuration, a peaking capacitor was connected in parallel with the flashboard chains and the 100nh inductors were removed in order to produce a faster discharge. The resultant plasma was not uniform. The light intensity measured by a 5ns framing camera was found to be a reasonable and reliable technique for qualitatively monitoring relative carbon plasma density and velocity of flow. Analysis of the frame pictures along with the parallel measurements done by emission spectroscopy gives very good agreement as to where there is carbon plasma.

*Work supported by the Plasma Physics Division, Naval Research Laboratory, Contract #N00014-90-J-2002 and Sandia National Laboratory Contract #63-4881.

- ☐ Prefer Poster Session
- ☐ Prefer Oral Session
- ☐ No Preference

Submitted by:

- ☐ This poster/oral should be placed in the following grouping: (specify order)

(Signature of APS Member)

D.A. HAMMER

(Same Name Typewritten)

- ☐ Special Facilities Requested (e.g., movie projector)

- ☐ Other Special Requests

(Address)

Abstract Submitted for the Thirty-second Annual Meeting
(Division of Plasma Physics)
November 12-16, 1990

Category Number and Subject 5.14

 Theory X Experiment

"Neutron Production in Dense X-Pinch Plasma with CD_2 Fibers," K.C. MITTAL, D.H. KALANTAR, N.QI, D.A. HAMMER, Cornell University, and J.D. SETHIAN, Naval Research Labs., - Dense Z-pinch experiments conducted at NRL¹ with frozen D_2 and CD_2 fibers have shown a neutron yield per pulse Y of up to 2×10^9 at current I of up to ~ 1 MA, apparently due to the onset of the $m = 0$ instability. Although Y appears to scale as I^{10} it may be impossible² for Y to exceed 10^{12} by increasing I . As an alternate approach, we are investigating the X-pinch configuration, in which a number of 50-100 micron CD_2 fibers will be mounted to cross at one or more points between the electrodes of the 0.5 TW, 40ns power pulse LION accelerator. Total neutron yield will be measured with rhodium foil activation counters and "bubble damaged" detectors as a function of I and specific configuration. Time dependent neutron production will be measured with scintillator/photo-multiplier detectors. Diagnostics available for plasma characterization include an x-ray pinhole camera, visible and x-ray streak cameras, XUV and x-ray spectrographs, and filtered photoconducting diodes. Results of the first experimental run will be presented.

* Work supported by Plasma Physics Division of the Naval Research Laboratory under Contract N00014-90-J-2002.

¹ J.D. Sethian, et al., 1990 IEEE Int'l. Conf. on Plasma Science, Conference Record 90CH2857-1, p. 105.

² G.H. McCall, Phys. Rev. Lett. **62**, 1986 (1989).

- ☐ Prefer Poster Session
- ☐ Prefer Oral Session
- ☐ No Preference

Submitted by:

- ☐ This poster/oral should be placed in the following grouping: (specify order)

(Signature of APS Member)

D.H. Hammer
(Same Name Typewritten)

- ☐ Special Facilities Requested (e.g., movie projector)

- ☐ Other Special Requests

(Address)

Abstract Submitted for the Thirty-second Annual Meeting
(Division of Plasma Physics)
November 12-16, 1990

Category Number and Subject 5.15.1

 Theory X Experiment

"Studies of a Long Conduction Time Plasma Opening Switch," L.K. ADLER, J.B. GREENLY and D.A. HAMMER, Cornell University,* - Plasma light from a long conduction time planar plasma opening switch¹ has been studied with a 5ns frame camera which viewed the switch region both side-on and end on. Viewed from the side, most of the current appears to be carried in a 1-2cm wide channel which moves from the generator end to the load end of the injected plasma during the conduction phase. Once the channel, which extends the full 10cm width of the injected plasma, reaches the load end of the plasma, its width decreases and the light disappears mid-gap. Although a small amount of load current appears very early in the conduction phase, the majority of the current reaches the load only after the light decreases substantially mid-gap. The correlation between light levels in the frames and measurements with a magnetic probe array will be presented.

*Work supported by the Plasma Physics Division, NRL, Washington, DC 20375-5000 under ONR contract N00014-90-J-2002.

¹L.K. Adler et al., Proceedings of the IEEE Plasma Science Conference, Oakland, CA, pg. 186-7.

- ☐ Prefer Poster Session
- ☐ Prefer Oral Session
- ☐ No Preference

Submitted by:

- ☐ This poster/oral should be placed in the following grouping: (specify order)

(Signature of APS Member)

D.A. HAMMER
(Same Name Typewritten)

- ☐ Special Facilities Requested (e.g., movie projector)

- ☐ Other Special Requests

(Address)

Abstract Submitted for the Thirty-second Annual Meeting
(Division of Plasma Physics)
November 12-16, 1990

Category Number and Subject 9.3 or 5.14

 Theory X Experiment

"Fluorescence Measurements for an Al/Mg Resonant Photo-Pumped X-Ray Laser Scheme," N. QI, D.A. HAMMER, D.H. KALANTAR, K.C. MITTAL, and G.J. BORDONARO, Cornell University. - An X-pinch, in which two Al wires cross at one or more points connecting the electrodes of a pulsed power source, has been imploded by the 0.5 TW LION accelerator with a 30ns rise time and ~500kA peak current. Bright and spatially confined bursts of x-ray radiation were observed from the wire crossing points. This source appears suitable as the pump for the AlXI-MgIX soft x-ray laser scheme.¹ A collisional radiative model which includes trapping was constructed to calculate the required conditions for the pump and laser plasmas. The required pump power of 0.2 GW in the 48.3Å AlXI line, derived by assuming the pump and lasing plasmas are 0.5cm apart, could be achieved with the ~ 10²⁰/cm³, ~400eV Al plasma we have obtained in our X-pinch experiments. In the fluorescence experiments, both the Al and Mg plasmas are imploded by the LION accelerator in several X-pinch configurations which can maintain the plasmas as close as 0.5cm apart. Fluorescence is measured by using a spatially resolved 1.0m grazing incident spectrograph.

* Work supported by the Plasma Physics Division, Naval Research Laboratory, Washington, DC 20375-5000, under ONR Contract N00014-89-J-2009.

¹M. Krishnan and J. Trebes, Appl. Phys. Lett. **45**, 189 (1984).

- ☐ Prefer Poster Session
- ☐ Prefer Oral Session
- ☐ No Preference

Submitted by:

- ☐ This poster/oral should be placed in the following grouping: (specify order)

(Signature of APS Member)

(Same Name Typewritten)

- ☐ Special Facilities Requested (e.g., movie projector)

- ☐ Other Special Requests

(Address)

Abstract Submitted for the Thirty-second Annual Meeting
(Division of Plasma Physics)
November 12-16, 1990

Category Number and Subject _____

___ Theory ___ Experiment

"X-pinch Soft X-ray Source Current Scaling," D.H. KALANTAR, L.A. BRISSETTE, D.A. HAMMER, Cornell University* and F.C. YOUNG, S.J. STEPHANAKIS, P.G. BURKHALTER, G. MEHLMAN, D.A. NEWMAN, Naval Research Laboratory - Following up on earlier¹ x-pinch x-ray source experiments on LION at Cornell (~500 kA peak, 80 ns fwhm current pulse), we have carried out experiments on Gamble II at NRL (0.8 - 1.0 MA peak, 90ns fwhm current pulse). From 2 to 4 aluminum wires ranging in size from 25 μ m to 100 μ m diameter were used to form the x-pinch load. X-ray diagnostics included a filtered XRD, photoconducting diodes (PCDs), a curved crystal spectrograph, a pinhole camera and a step-filtered x-ray film camera. Preliminary analysis of the PCD data indicates about 20 times as much Al K-shell energy at 800 kA on Gamble II, and about 40 times as much at 1 MA, as at 450 kA on LION. The Gamble II yield increased with decreasing wire mass as the K-shell emission started earlier in the pulse. However, the K-shell source region increased in size from ≤ 0.5 mm on LION to an effective size of a few mm on Gamble II. At 800 kA, absolute energy estimates from the various diagnostics ranged from about 80J to a few hundred J. Initial results from a new run on LION will also be presented.

*Research supported by NSF and Plasma Physics Division, NRL.

¹ D.H. Kalanter et al., Bull. Am. Phys. Soc. 34, 1945 (1989).

☐ Prefer Poster Session

Submitted by:

☐ Prefer Oral Session

☐ No Preference

☐ This poster/oral should be placed in the following grouping: (specify order)

(Signature of APS Member)

(Same Name Typewritten)

☐ Special Facilities Requested (e.g., movie projector)

☐ Other Special Requests

(Address)

November 16-20, 1992, Seattle, WA

X Theory	Experiment
----------	------------

1. G. Z. Sun et al, Phys. Fluids, **30**, 526 (1987).
2. T. Kurki-Suonio et al, Phys. Rev. A, **40**, 3230 (1989).
3. P. Sprangle et al, Phys. Rev. A, **41**, 4463 (1990); A. Ting et al, Phys. Fluids, **B2**, 1390 (1990).
4. P. K. Kaw et al, Phys. Rev. Lett., **68**, 3172 (1992).

- Submitted by:

Am Ende

(Signature of APS Member)

R. N. Sudan

(Same Name Typewritten)

**369 Upson Hall
Cornell Univeristy
Ithaca, N.Y. 14850**

(Address)

X-PINCH SOFT X-RAY SOURCE FOR MICROLITHOGRAPHY

S.C. Glidden, D.A. Hammer, D.H. Kalantar, and N. Qi

Laboratory of Plasma Studies, Cornell University, Ithaca, NY 14853

and

Applied Pulsed Power, Inc., 140 Langmuir Lab., 95 Brown Rd., Ithaca, NY 14850

Abstract

The x-pinch soft x-ray source is described for application in submicron resolution lithography. Experiments have been performed to characterize the radiation emitted from magnesium wire x-pinch plasmas using an 80 ns, ≤ 500 kA pulse. Yields of 14.2 J averaged over three independent calibrated diagnostics at 445 kA have been measured in magnesium K-shell radiation (predominantly 8.4 Å to 9.4 Å or 1.5 keV to 1.3 keV) from a submillimeter source, with as little as 5-10% of the yield below the 6.74 Å silicon absorption edge. A new ≤ 700 kA, 100 ns pulser being used for x-pinch physics experiments is described. The design of a 40 pulse per second pulsed power system and wire loading mechanism for exposing a resist in 1 second at a distance of 40 cm is presented.

I. Introduction

In this paper we describe the work at Cornell on the x-pinch plasma soft x-ray source, and the design of a compact, high repetition rate pulser at Applied Pulsed Power, Inc. (APP), for practical testing of the x-pinch for application to lithography in the microelectronics industry. A close relative to the conventional wire-array z-pinch, the x-pinch consists of two or more wires stretched between the output electrodes of a pulsed power generator in an 'X' configuration so that they touch at a single point, as illustrated in Fig. 1. The current pulse from the pulsed power generator causes a plasma to form at the initial position of the wires in a few ns, and the self-magnetic field causes the plasma to pinch towards the axis. Because the current is shared by several wires except at the single point where they touch, only there is the plasma implosion powered by the full current, thereby generating intense soft x-ray radiation only at that point. Using magnesium (Mg) wires in the x-pinch, the radiation is mostly K-shell lines between 8.4 Å and 9.4 Å, an attractive range for x-ray lithography.¹

Although our experiments to date^{2,3} suggest that the scientific feasibility of the Mg x-pinch for microlithography is established, as described in Sections II-IV, studies are continuing to understand the physics of the x-pinch. Taking advantage of a pulser built especially for x-pinch experiments, which is described in Section V, these studies will enable us to optimize the x-pinch for the lithography application. Considerations which led us to choose a 40 pulses per second, 500 kA pulser for a prototype lithography system are also discussed in Section IV, and the pulser design itself is presented in Section VI.

II. Experimental Procedure

The x-pinch experiments were conducted using the LION pulsed power generator⁴ to deliver up to a 470 kA, 80 ns full width at half maximum (fwhm) current pulse to the crossed wire loads. Experiments were